University of Messina

Department of Biomedical, Dental, Morphological and Functional Imaging Sciences

PhD in Translational Molecular Medicine and Surgery

Cycle XXXV

Coordinator: Professor Gaetano Caramori

SSD: MED/04

Evaluation of SARS-CoV-2 genomic mutations potentially conferring resistance to antiviral drugs in viral populations isolated from untreated SARS-CoV-2 - infected subjects

PhD student:

Giuseppe Caminiti

Tutor:

Professor Teresa Pollicino

Academic year 2021-2022

Index

Introduction

The development of safe and effective antiviral drugs was a crucial topic since the outbreak of Severe Acute Respiratory Syndrome Coronavirus-2 (SARS-CoV-2) global pandemic and – despite the extensive vaccination campaign – it is still critical for people who do not respond robustly to vaccination, can't be vaccinated or have not been vaccinated for non-clinical reasons [1, 2]. Among the drugs tested for treatment of SARS-CoV-2 infected patients, the nucleoside analog Remdesivir (brand name Veklury) was the first to be approved for the treatment of Coronavirus virus disease 2019 (COVID-19) by the Food and Drug Administration (FDA) [3] and the European Medicines Agency (EMA) [4]. The target of Remdesivir is the non-structural protein 12 (Nsp12), which is the catalytic subunit of the RNA-dependent RNA polymerase (RdRp) complex [1,5]. SARS -CoV-2 genome replication and transcription are based on the function of the RdRp complex, which is composed by the catalytic subunit nsp12, and the two accessory subunits nsp7 and nsp8 [6]. The nsp12 [amino acid (aa) S367 - F920] subunit includes an N-terminal nidovirus RdRp-associated nucleotidyl-transferase (NiRAN) domain, an interface domain, and a C-terminal RdRp domain [7]. The RdRp looks like a right hand, comprises the fingers (residues L366 - A581 and K621 -G679), palm (from residues T582 to P620 and T680 to Q815), and thumb (residue H816 to F920) subdomains. Subunits nsp7 and nsp8 bind to the thumb, and an additional copy of nsp8 binds to the finger domain [7]. Remdesivir can bypass the proofreading activity of SARS-CoV-2, since its incorporation does not stop elongation but only blocks RdRp after the extension with three additional nucleotides [5, 8, 9]. Another drug recently approved by the United Kingdom's Medicines Regulator [10] and FDA [11] for the treatment of patients with COVID-19 is Molnupiravir (also known as MK 4482 or Lagrevio), which also targets the RdRp of SARS-CoV-2. In comparison to Remdesivir that is administered by infusion, Molnupiravir is orally bioavailable. This compound acts as a mutagenizing agent that lead to an 'error catastrophe' during viral replication [12, 13]. A third arrow in the quiver of antiviral drugs was recently added with the approval of Nirmatrelvir and ritonavir combination (Paxlovid) [14, 15]. Paxlovid is an orally bioavailable drug like Molnupiravir, which can be administered at the first sign of SARS-CoV-2 infection and can potentially help patients to avoid severe illness, hospitalization and death. Unlike Remdesivir and Molnupiravir, Paxlovid is designed to block the activity of SARS-CoV-2 Nsp5/Main Protease (Mpro)/3C-like protease (3CLpro). Nsp5 structure includes a chymotrypsin-like domain (domain I, residues 8–101), a 3C protease-like (domain II, residues 102–184) and globular domain (domain III, residues 201–303), responsible of the dimerization of two distinct protomers of nsp5 [16, 17]. The dimerization of two protomers results in the formation of a catalytic site for each protomer, where C145 and H41 represent the catalytic

residues [16, 17]. Nsp5 is responsible of the maturation of non-structural proteins including those of the RdRp complex [18]. Therefore, Paxlovid inhibits viral replication acting upstream the replication complex itself [19].

Given the adaptive potential of SARS-Cov-2 and the ongoing selection of viral variants that display some degree of resistance to vaccines, it is conceivable that natural selection of mutant viruses might also jeopardize the efficacy of new developed antiviral agents.

Identification and transmission prevention of potential antiviral resistant SARS-CoV-2 variants is essential for infection surveillance. Non-synonymous variants in nsp12 have been reported in two studies from different countries (P323L nsp12 substitution) [20, 21] and in a single case associated with clinical failure of Remdesivir treatment (D484Y nsp12 substitution) [22]. Furthermore, recent in vitro studies have shown that the amino acid substitutions F480L, V557L and E802D in nsp12 may reduce the sensitivity of SARS-CoV-2 to Remdesivir [23]. At the moment no Molnupiravir nor Paxlovid resistance-associated amino acid substitutions were identified, although clinical and cell culture studies have not been completed. Therefore, aim of this study was to analyze the prevalence of SARS-CoV-2 variants and the genetic variability of the RdRp complex subunits and Nsp5 in SARS-Cov-2 populations isolated from a large series of subjects naïve to antiviral therapy.

Materials and methods

Samples

A total of 4155 nasopharyngeal swabs from subjects with a first-time positive SARS-CoV-2 PCR test were analyzed at the Molecular Diagnostic Laboratory of the Division of Advanced Diagnostic Laboratories – University Hospital "G. Martino" of Messina, Italy – from April 2021 to October 2022. The Molecular Diagnostic Laboratory is one of the regional reference laboratories across Italy for the identification of the SARS-CoV-2 emerging variants in Italy. Data collected in this study had the primary purpose of providing a health service, therefore ethical approval was not required for this study.

Viral nucleic acid extraction

The viral RNA extraction was performed using the automated nucleic acid purification platform Maxwell RSC 48 (Promega Corporation, Madison, Wisconsin, USA) and the Maxwell RSC Viral TNA kit (Promega Corporation, Madison, Wisconsin, USA) following the manufacturer's instruction.

Next-Generation-Sequencing (NGS) analysis of SARS-CoV-2 isolates

Viral RNA reverse transcription, cDNA amplification and construction of libraries were performed using the QIAseq DIRECT SARS CoV-2 kit (Qiagen, Hilden, Germany) following the manufacturer's instruction. The prepared libraries were then sequenced using MiSeq platform producing 151bp paired-end reads (Illumina, San Diego, California, USA).

Bioinformatic analysis

The SARS-CoV-2 complete genomes were reconstructed using the pipeline SARS-CoV-2 RECoVERY (REconstruction of COronaVirus gEnomes & Rapid analYsis) [24]. Finally, the consensus sequences were analyzed using Aliview program (v1.27), to identify the mutations in the *nsp5, 7, 8* and *12* genes.

Phylogenetic analysis

To obtain information on phylogenetic relationship among viral isolates, Molecular Evolutionary Genetics Analysis X (MEGAX) [25] with the Muscle algorithm was applied to re-align consensus sequences of *nsp5, nsp7, nsp8* and *nsp12* genes and to construct the phylogenetic tree. The evolutionary history was inferred by using the Maximum Likelihood method and Tamura-Nei [26], with default parameters. The bootstrap consensus tree was inferred from 500 replicates and was used to represent the evolutionary history of the virus analyzed [27]. The output tree was visualized using the online tool, Interactive Tree of Life (iTOL) [28].

Results

SARS-CoV-2 Lineage Analysis

NGS analysis of the 4155 nasopharyngeal swabs showed that 2957 (71.2%) viral genomes belonged to B.1.617.2 (Delta) variant, 924 (22.2%) to B.1.1.529 (Omicron) variant, 250 (6%) to B.1.1.7 (Alpha) variant, while the remaining 24 (0.6%) belonged to SARS-CoV-2 variants that were less common in our geographic area (**Figure 1**). The obtained results are essentially due to the fact that NGS analysis of SARS-CoV-2 variants was started at the Molecular Diagnostic Laboratory of the University Hospital of Messina, Italy, at the beginning of April 2021. At that time, the prevalence of the Alpha variant reached 88.8% of the cases. In eastern Sicily, the Delta variant was detected in SARS-Cov-2 infected cases from June 2021onwards making up almost 100% of sequenced Covid-19 cases in October 2021. Two months later the Omicron variant accounted for 17% of total COVID-19 cases. Soon after, Omicron overcame the Delta variant accounting for 77 % of the cases in January 2022 and for 93.5% of the cases one month later. From March 2022 until today, the Omicron variant and parent lineages have represented 100% of the cases (**Table 1, Figure 2**).

NGS and bioinformatic analysis

SARS-CoV-2 RdRp complex

Catalytic subunit

Analysis of the *nsp12* genomic sequence led to identify several aa substitutions located into the five domains of the nsp12 protein (**Figure 3**). The aa substitutions with the most elevated prevalence into the NiRAN domain where A46S and R197Q, detected in 17/4155 (0.4%) and 104/ 4155 (2.5%) of the samples, respectively. All the viral genomes harboring these substitutions belonged to the Delta variant and parent lineages, while 2/924 (0.2%) of the viral genomes belonging to Omicron variant showed the N215D substitution.

The interface domain, which connects the NiRAN domain to the polymerase domain [7], harbored the P323L substitution that was detected in 3777/4155 (91%) of the samples. A total of 219/3777 (5.8%) of the isolates harbor ring the P323L belongs to Alpha variant, 2615/3777 (69.2%) to Delta variant and parent lineages, while 921/3777 (24.4%) to Omicron variant and parent lineages. The remaining 22/3777 (0.6%) the samples belong to other variants [1 to B.1.351 (Beta), 11 to the P.1 (Gamma), 2 to B.1.525 (Eta), 1 to P.3 (Theta), 5 to C.37 (Lambda) variant, respectively). The polymerase domain is composed by three subdomains: fingers subdomain, palm subdomain and thumb subdomain [7]. Concerning the fingers subdomains, sequencing analysis identified the

M463I, V472L and A656V substitutions respectively in 25/4155 (0.6%), 34/4155 (0.8%) and 20/4155 (0.5%) all belonging to Delta variant and parent lineages. The G671S substitution was detected in 2906/4155 (69.9%) of the isolated SARS-CoV-2 genomes, 2904/4155 (99.05%) belong to Delta variant, while 2/4155 (0.05%) belong to Omicron BA.5, a sub-variant. The palm subdomain harbored the A716V and the D804N substitutions. The A716V substitution was detected in 16/4155 (0.4%) of the isolates (all belonging to the Alpha variant), whereas the D804N substitution was detected in 26/4155 (0.6%) of cases (all belonging to Delta and parent lineages).

Concerning the thumb subdomain, 457/4155 (11%) of the samples showed the L838I substitution. Other mutations detected into the thumb subdomain were the Q822H and the D824Y substitutions [6, 29, 30] and deletion of aa 908 (T908del), detected in 140/4155(3.4%), 21/4155 (0.5%) and 26/4155 (0.6%) of the samples, respectively. These four mutations in the thumb subdomain were only detected in Delta variant and parent lineages. Notably, the D484Y substitution that has been detected in patients who failed Remdesivir treatment [22] and the E802D substitution that may reduce the sensitivity to remdesivir *in vitro* [23], were not detected in any of the isolated SARS-CoV-2 genomes. All the aa substitutions identified in Nsp12 subunit are reported in **Table 2a and 2b**.

Accessory subunits

Sequencing analysis of the *nsp7* and *nsp8* genomic regions identified respectively 14 and 24 aa substitutions at very low frequency (**Figure 3**). In particular, among the 14 aa substitutions identified in the nsp7 subunit, the L56F substitution was the one detected at higher frequency [16/4155 (0.4%) of the isolated genomes] (**Table 3a and 3b**). Furthermore, among the 24 aa substitution identified in the nsp8 subunit, the M55I and the T148I substitutions were the ones that showed higher frequency [34/4155 (0.82%) and 33/4155 (0.79%), respectively]. (**Table 4a and 4b**)

Nsp5

Sequencing analysis of nsp5 led to identify 28 aa substitutions located into the three domains of the protein (**Figure 3, Table 5a and 5b**). K90R, P132H and V186F are the aa substitutions that showed higher frequency (118/4155 (2.8%), 648/4155 (15.6%) and 157/4155 (3.8%) of the cases, respectively). All the samples harboring the P132H substitution belonged to the Omicron variant and parent lineages, while those with the V186F belonged to the Delta variant and parent lineages. The K90R substitution was common to both Omicron and Delta variant as well as to other lineages (**Table 5a and 5b**). Furthermore, though at very low prevalence [3/4155 (0.07%) of the cases], the A191V substitution was also detected. This mutation is of potential interest since it affects one of the amino acids flanking the catalytic site of nsp5 [16].

Phylogenetic analysis

Concerning *nsp*12 and *nsp*5, phylogenetic analysis showed that variants harboring the same pattern of amino acid substitutions clustered into the same clade. The presence of single nucleotide mutations caused the further subdivision of the clades in different subgroups (**Figure 4, 5, 6 and 7**). Concerning *nsp*7 and *nsp*8, phylogenetic analysis evidenced the low variability of these two regions. Indeed, sequences of Alpha, Delta, and Omicron variants (including their parent lineages) clustered together.

Discussion

The first two antiviral drugs approved for the treatment of SARS-CoV-2 are Remdesivir [3, 4] and Molnupiravir [10, 11]. Both the compounds target nsp12, the catalytic subunit of the RdRp complex, inhibiting replication and transcription of SARS-CoV-2 [5, 31, 32]. The fast and global spread of SARS-CoV-2 resulted in the rapid selection and emergence of different viral variants and lineages that may harbor aa substitutions affecting the effectiveness of antiviral therapy [20-23]. These substitutions can be naturally selected, such as the E802D – the only spontaneous substitution known to reduce the sensitivity to Remdesivir *in vitro* [23] – or emerge in response to antiviral therapy, such as the D484Y – the only substitution detected after Remdesivir administration that has been associated with treatment failure [22]. Molnupiravir, similarly to Remdesivir, can bypass the proofreading exoribonuclease activity of SARS-CoV-2. However, to date no mutation inducing viral-resistance to Molnupiravir has been described [2]. In this study, we identified several mutations in SARS-CoV-2 genomic regions targeted by antiviral drugs. However, neither the E802D nor the D484Y aa substitution was identified. This may likely be due to the fact that all the studied samples were collected from subjects naïve to antiviral treatment.

The aa substitution that showed the highest prevalence (91% of the samples) was P323L. This result is consistent with prevalence data from North America, India and Europe [34, 35]. P323 is located into the interface domain (residues A250 to R365) [6], which strictly interact with nsp8 in the regulation of RNA synthesis [35, 36]. The substitution of a non-polar amino acid, such as proline, with a hydrophobic residue such as leucine increases the hydrophobic interaction between nsp12 and nsp8, possibly further enhancing the processivity of the RNA synthesis by the RdRp complex. Thus, the P323L substitution may have contributed to promote the epidemiological spread of the Omicron variant [20, 37]. However, the large diffusion of this variant would not necessarily have a negative impact on antiviral therapy, considering that a recent study suggested that the P323L substitution increases the affinity of nsp12 to Remdesivir, resulting in a greater effectiveness of the treatment [38].

The G671S substitution was detected from the first decade of July. Since then, the prevalence of G671S reached 99.8% of the cases in November 2021 and decreased to 5.8% in February 2022, mirroring the prevalence of Delta variant. The G671S substitution was not detected from March onward, with the exception of 2 samples belonging to Omicron BA.5 sub-variant. (**Table 2a and 2b**). We also detected the M463I, V472L, and A656V substitutions, which showed a very low prevalence (0.6%, 0.8% and 0.5% of the samples, respectively). It is currently unknown if these substitutions may have an impact on the effectiveness of antiviral drugs. Among the detected aa

substitutions, Q822H, D824Y and L838I were detected from the last decade of July. These substitutions are all located into the thumb domain of nsp12 and are involved in the interaction with nsp7-nsp8 heterodimer. Their prevalence was 3.4%, 0.5% and 11% of the samples, respectively (**Table 2a and 2b**). According to biochemical studies, the Q822H and D824Y substitutions may increase the rigidity of nsp12, thus affecting the efficiency of the whole viral replication complex [29, 30]. Notably, the prevalence of D824Y decreased over time and completely disappeared in October 2022, suggesting that a modification of nsp12 structure possibly is detrimental for the virus. The Q822H substitution disappeared in January 2022 simultaneously with the increased prevalence of Omicron variant. The effect of the L838I substitutions on the RdRp complex and the efficacy of antiviral drugs is still undetermined. The prevalence of L838I reached 27.4% in August 2021, decreased to 12.1% one month later and disappeared in February 2022 with the appearance of Omicron variant (**Table 2a and 2b**).

In this study both nsp7 and nsp8 showed an extremely low genetic variability. The T148I substitution in nsp8 showed the highest prevalence (0.8% of the samples) (**Table 3a, 3, 4a, and 4b**). Indeed, phylogenetic analysis demonstrated that both nsp7 and nsp8 sequences of evolutionally distant lineages clustered together, thus emphasizing that these genes are more conserved compared to nsp12 and nsp5 **(Figures 4, 5, 6 and 7).** Considering the important role of these two cofactors in increasing the efficiency of polymerization reaction [35, 36] and that both are less prone than nsp12 to accumulate aa substitutions, it is plausible to consider nsp7 and nsp8 as possible antiviral drugs targets.

The third antiviral drug that has been approved for the treatment of Covid-19 is Paxlovid, which targets the SARS-CoV-2 nsp5 main protease. In the present study no aa substitution has been identified in the active site of nsp5. The V186F substitution has been detected in 157/4155 (3.8%). Furthermore, A191V substitution, affecting one of the residues flanking the active site cavity, has been detected in 3/4155 (0.07%) of the samples (**Table 5a and 5b**). The presence of two aa substitutions close to the active site of nsp5 suggests that mutations conferring resistance to Paxlovid could be selected

CONCLUSIONS

On March 2020, the World Health Organization (WHO) declared COVID-19 outbreak a global pandemic [39]. To date vaccination is the most effective strategy against SARS-CoV-2 infection. However, it must be considered that none of the current vaccines shows 100% efficacy against symptomatic and severe COVID-19 disease [40-42]. Results from this study suggest that nsp7 and nsp8 might be considered as new potential target for the development of new antiviral drugs because of their low genetic variability and essential role in SARS-CoV-2 replication [7]. To date, only nsp12 and nsp5 has been targeted by antiviral therapies. However, both proteins may show aa substitutions, which emerged either spontaneously or in response to therapy that can reduce the efficacy to treatments. This study shows that both nsp12 and nsp5 may accumulate several naturally selected aa substitutions, which may potentially affect antiviral drug efficiency. However, most of these substitutions are still poorly characterized. Certain substitutions, such as the P323L in the nsp12, could increase the effectiveness of antiviral treatment [38] whereas other substitutions may overcome drug selective pressure. The natural selection of aa mutations may lead to the emergence of resistant SARS-CoV-2 variants that could compromise the efficacy of new developed antiviral compounds [5, 43]. In this regard, sequencing analysis will be crucial in the monitoring of RdRp complex and nsp5 variability. Furthermore, NGS analysis should be flanked by functional analysis studies in order to evaluate the impact of the detected mutations on antiviral treatment. This is of particular importance if one takes into consideration that we are going towards a future where antiviral drugs will be administrated more frequently for the treatment of Covid-19.

References

1. Tao K, Tzou PL, Nouhin J, Bonilla H, Jagannathan P, Shafer RW. SARS-CoV-2 Antiviral Therapy. Clin Microbiol Rev. 2021 Dec 15;34(4):e0010921. doi: 10.1128/CMR.00109-21. Epub 2021 Jul 28. PMID: 34319150; PMCID: PMC8404831.
2. Malone B, Campbell EA. Molnupiravir: coding for catastrophe. Nat Struct Mol Biol. 2021 Sep;28(9):706-708. doi: 10.1038/s41594-021-00657-8. Erratum in: Nat Struct Mol Biol. 2021 Nov;28(11):955. PMID: 34518697.
3. Rubin D, Chan-Tack K, Farley J, Sherwat A. FDA Approval of Remdesivir - A Step in the Right Direction. N Engl J Med. 2020 Dec 31;383(27):2598-2600. doi: 10.1056/NEJMp2032369. Epub 2020 Dec 2. PMID: 33264539.
4. Wise J. Covid-19: Remdesivir is recommended for authorisation by European Medicines Agency. BMJ. 2020 Jun 29;369:m2610. doi: 10.1136/bmj.m2610. PMID: 32601048.
5. Vicenti I, Zazzi M, Saladini F. SARS-CoV-2 RNA-dependent RNA polymerase as a therapeutic target for COVID-19. Expert Opin Ther Pat. 2021 Apr;31(4):325-337. doi: 10.1080/13543776.2021.1880568. Epub 2021 Mar 3. PMID: 33475441; PMCID: PMC7938656.
6. Hillen HS, Kokic G, Farnung L, Dienemann C, Tegunov D, Cramer P. Structure of replicating SARS-CoV-2 polymerase. Nature. 2020 Aug;584(7819):154-156. doi: 10.1038/s41586-020-2368-8. Epub 2020 May 21. PMID: 32438371.
7. Gao Y, Yan L, Huang Y, Liu F, Zhao Y, Cao L, Wang T, Sun Q, Ming Z, Zhang L, Ge J, Zheng L, Zhang Y, Wang H, Zhu Y, Zhu C, Hu T, Hua T, Zhang B, Yang X, Li J, Yang H, Liu Z, Xu W, Guddat LW, Wang Q, Lou Z, Rao Z. Structure of the RNA-dependent RNA polymerase from COVID-19 virus. Science. 2020 May 15;368(6492):779-782. doi: 10.1126/science.abb7498. Epub 2020 Apr 10. PMID: 32277040; PMCID: PMC7164392.
8. Kokic G, Hillen HS, Tegunov D, Dienemann C, Seitz F, Schmitzova J, Farnung L, Siewert A, Höbartner C, Cramer P. Mechanism of SARS-CoV-2 polymerase stalling by remdesivir. Nat Commun. 2021 Jan 12;12(1):279. doi: 10.1038/s41467-020-20542-0. PMID: 33436624; PMCID: PMC7804290.
9. Bravo JPK, Dangerfield TL, Taylor DW, Johnson KA. Remdesivir is a delayed translocation inhibitor of SARS-CoV-2 replication. Mol Cell. 2021 Apr 1;81(7):1548-1552.e4. doi: 10.1016/j.molcel.2021.01.035. Epub 2021 Jan 28. PMID: 33631104; PMCID: PMC7843106.
10. Regulatory approval of Lagevrio (molnupiravir). https://www.gov.uk/government/publications/regulatory-approval-of-lagevrio-molnupiravir.

11. Food and Drug Administration. Coronavirus (covid-19) update: FDA authorizes additional oral antiviral for treatment of covid-19 in certain adults. Press release, 23 Dec 2021. https://www.fda.gov/news-events/press-announcements/coronavirus-covid-19-update-fda-authorizes-additional-oral-antiviral-treatment-covid-19-certain
12. Kabinger F, Stiller C, Schmitzová J, Dienemann C, Kokic G, Hillen HS, Höbartner C, Cramer P. Mechanism of molnupiravir-induced SARS-CoV-2 mutagenesis. Nat Struct Mol Biol. 2021 Sep;28(9):740-746. doi: 10.1038/s41594-021-00651-0. Epub 2021 Aug 11. PMID: 34381216; PMCID: PMC8437801.
13. Mahase E. Covid-19: Molnupiravir reduces risk of hospital admission or death by 50% in patients at risk, MSD reports. BMJ. 2021 Oct 4;375:n2422. doi: 10.1136/bmj.n2422. PMID: 34607801.
14. Food and Drug Administration. Coronavirus (covid-19) update: FDA Authorizes First Oral Antiviral for Treatment of COVID-19. Press release, December 22, 2021. https://www.fda.gov/news-events/press-announcements/coronavirus-covid-19-update-fda-authorizes-first-oral-antiviral-treatment-covid-19
15. European Medici Agency. COVID-19: EMA recommends conditional marketing authorisation for Paxlovid. Press release, 27 01 2022.
16. Kneller DW, Phillips G, O'Neill HM, Jedrzejczak R, Stols L, Langan P, Joachimiak A, Coates L, Kovalevsky A. Structural plasticity of SARS-CoV-2 3CL Mpro active site cavity revealed by room temperature X-ray crystallography. Nat Commun. 2020 Jun 24;11(1):3202. doi: 10.1038/s41467-020-16954-7. PMID: 32581217; PMCID: PMC7314768.
17. Lee J, Worrall LJ, Vuckovic M, Rosell FI, Gentile F, Ton AT, Caveney NA, Ban F, Cherkasov A, Paetzel M, Strynadka NCJ. Crystallographic structure of wild-type SARS-CoV-2 main protease acyl-enzyme intermediate with physiological C-terminal autoprocessing site. Nat Commun. 2020 Nov 18;11(1):5877. doi: 10.1038/s41467-020-19662-4. PMID: 33208735; PMCID: PMC7674412.
18. Mahase E. Covid-19: Pfizer's paxlovid is 89% effective in patients at risk of serious illness, company reports. BMJ. 2021 Nov 8;375:n2713. doi: 10.1136/bmj.n2713. PMID: 34750163.
19. Jin Z, Du X, Xu Y, Deng Y, Liu M, Zhao Y, Zhang B, Li X, Zhang L, Peng C, Duan Y, Yu J, Wang L, Yang K, Liu F, Jiang R, Yang X, You T, Liu X, Yang X, Bai F, Liu H, Liu X, Guddat LW, Xu W, Xiao G, Qin C, Shi Z, Jiang H, Rao Z, Yang H. Structure of Mpro from SARS-CoV-2 and discovery of its inhibitors. Nature. 2020 Jun;582(7811):289-293. doi: 10.1038/s41586-020-2223-y. Epub 2020 Apr 9. PMID: 32272481.

20. Pachetti M, Marini B, Benedetti F, Giudici F, Mauro E, Storici P, Masciovecchio C, Angeletti S, Ciccozzi M, Gallo RC, Zella D, Ippodrino R. Emerging SARS-CoV-2 mutation hot spots include a novel RNA-dependent-RNA polymerase variant. J Transl Med. 2020 Apr 22;18(1):179. doi: 10.1186/s12967-020-02344-6. PMID: 32321524; PMCID: PMC7174922.
21. Eskier D, Suner A, Karakülah G, Oktay Y. Mutation density changes in SARS-CoV-2 are related to the pandemic stage but to a lesser extent in the dominant strain with mutations in spike and RdRp. PeerJ. 2020 Aug 19;8:e9703. doi: 10.7717/peerj.9703. PMID: 32879797; PMCID: PMC7443079.
22. Martinot M, Jary A, Fafi-Kremer S, Leducq V, Delagreverie H, Garnier M, Pacanowski J, Mékinian A, Pirenne F, Tiberghien P, Calvez V, Humbrecht C, Marcelin AG, Lacombe K. Emerging RNA-Dependent RNA Polymerase Mutation in a Remdesivir-Treated B-cell Immunodeficient Patient With Protracted Coronavirus Disease 2019. Clin Infect Dis. 2021 Oct 5;73(7):e1762-e1765. doi: 10.1093/cid/ciaa1474. PMID: 32986807; PMCID: PMC7543308.
23. Szemiel AM, Merits A, Orton RJ, MacLean OA, Pinto RM, Wickenhagen A, Lieber G, Turnbull ML, Wang S, Furnon W, Suarez NM, Mair D, da Silva Filipe A, Willett BJ, Wilson SJ, Patel AH, Thomson EC, Palmarini M, Kohl A, Stewart ME. In vitro selection of Remdesivir resistance suggests evolutionary predictability of SARS-CoV-2. PLoS Pathog. 2021 Sep 17;17(9):e1009929. doi: 10.1371/journal.ppat.1009929. Epub ahead of print. PMID: 34534263.
24. Luca De Sabato, Gabriele Vaccari, Arnold Knijn, Giovanni Ianiro, Ilaria Di Bartolo, Stefano Morabito. SARS-CoV-2 RECoVERY: a multi-platform open-source bioinformatic pipeline for the automatic construction and analysis of SARS-CoV-2 genomes from NGS sequencing data. bioRxiv 2021.01.16.425365; doi: https://doi.org/10.1101/2021.01.16.425365
25. Kumar S, Stecher G, Li M, Knyaz C, Tamura K. MEGA X: Molecular Evolutionary Genetics Analysis across Computing Platforms. Mol Biol Evol. 2018 Jun 1;35(6):1547-1549. doi: 10.1093/molbev/msy096. PMID: 29722887; PMCID: PMC5967553.
26. Tamura K, Nei M. Estimation of the number of nucleotide substitutions in the control region of mitochondrial DNA in humans and chimpanzees. Mol Biol Evol. 1993 May;10(3):512-26. doi: 10.1093/oxfordjournals.molbev.a040023. PMID: 8336541.
27. Felsenstein J. Confidence limits on phylogenies: an approach using the bootstrap. Evolution. 1985 Jul;39(4):783-791. doi: 10.1111/j.1558-5646.1985.tb00420.x. PMID: 28561359.

28. Letunic I, Bork P. Interactive Tree Of Life (iTOL) v5: an online tool for phylogenetic tree display and annotation. Nucleic Acids Res. 2021 Jul 2;49(W1):W293-W296. doi: 10.1093/nar/gkab301. PMID: 33885785; PMCID: PMC8265157.
29. Tokgun O, Caliskan A, Coskun C, Tokgun PE, Akca H. Whole Genome Sequencing and Phylogenetic Analysis of SARS-CoV-2 strains in Turkey. J Infect Dev Ctries. 2021 Apr 30;15(4):470-477. doi: 10.3855/jidc.14560. PMID: 33956645.
30. Yashvardhini N, Jha DK, Bhattacharya S. Identification and characterization of mutations in the SARS-CoV-2 RNA-dependent RNA polymerase as a promising antiviral therapeutic target. Arch Microbiol. 2021 Aug 19:1–11. doi: 10.1007/s00203-021-02527-9. Epub ahead of print. PMID: 34410443; PMCID: PMC8374121.
31. Pushpakom S, Iorio F, Eyers PA, Escott KJ, Hopper S, Wells A, Doig A, Guilliams T, Latimer J, McNamee C, Norris A, Sanseau P, Cavalla D, Pirmohamed M. Drug repurposing: progress, challenges and recommendations. Nat Rev Drug Discov. 2019 Jan;18(1):41-58. doi: 10.1038/nrd.2018.168. Epub 2018 Oct 12. PMID: 30310233.
32. De Farias ST, Dos Santos Junior AP, Rêgo TG, José MV. Origin and Evolution of RNA-Dependent RNA Polymerase. Front Genet. 2017 Sep 20;8:125. doi: 10.3389/fgene.2017.00125. PMID: 28979293; PMCID: PMC5611760.
33. Wang, R.; Hozumi, Y.; Yin, C.; Wei, G.W. Decoding SARS-CoV-2 Transmission and Evolution and Ramifications for COVID-19 Diagnosis, Vaccine, and Medicine. J. Chem. Inf. Model. 2020.
34. Chand, G.B.; Banerjee, A.; Azad, G.K. Identification of novel mutations in RNA-dependent RNA polymerases of SARS-CoV-2 and their implications on its protein structure. PeerJ 2020, 8, e9492.
35. Reshamwala SMS, Likhite V, Degani MS, Deb SS, Noronha SB. Mutations in SARS-CoV-2 nsp7 and nsp8 proteins and their predicted impact on replication/transcription complex structure. J Med Virol. 2021 Jul;93(7):4616-4619. doi: 10.1002/jmv.26791. Epub 2021 Mar 14. PMID: 33433004; PMCID: PMC8012999.
36. Peng Q, Peng R, Yuan B, Zhao J, Wang M, Wang X, Wang Q, Sun Y, Fan Z, Qi J, Gao GF, Shi Y. Structural and Biochemical Characterization of the nsp12-nsp7-nsp8 Core Polymerase Complex from SARS-CoV-2. Cell Rep. 2020 Jun 16;31(11):107774. doi: 10.1016/j.celrep.2020.107774. Epub 2020 May 30. PMID: 32531208; PMCID: PMC7260489.
37. Ilmjärv, S., Abdul, F., Acosta-Gutiérrez, S. et al. Concurrent mutations in RNA-dependent RNA polymerase and spike protein emerged as the epidemiologically most successful

SARS-CoV-2 variant. Sci Rep 11, 13705 (2021) https://doi.org/10.1038/s41598-021-91662-w

38. Mohammad A, Al-Mulla F, Wei DQ, Abubaker J. Remdesivir MD Simulations Suggest a More Favourable Binding to SARS-CoV-2 RNA Dependent RNA Polymerase Mutant P323L Than Wild-Type. Biomolecules. 2021 Jun 22;11(7):919. doi: 10.3390/biom11070919. PMID: 34206274; PMCID: PMC8301449.
39. Cucinotta D, Vanelli M. WHO Declares COVID-19 a Pandemic. Acta Biomed. 2020 Mar 19;91(1):157-160. doi: 10.23750/abm.v91i1.9397. PMID: 32191675; PMCID: PMC7569573.
40. Tartof SY, Slezak JM, Fischer H, Hong V, Ackerson BK, Ranasinghe ON, Frankland TB, Ogun OA, Zamparo JM, Gray S, Valluri SR, Pan K, Angulo FJ, Jodar L, McLaughlin JM. Effectiveness of mRNA BNT162b2 COVID-19 vaccine up to 6 months in a large integrated health system in the USA: a retrospective cohort study. Lancet. 2021 Oct 16;398(10309):1407-1416. doi: 10.1016/S0140-6736(21)02183-8. Epub 2021 Oct 4. PMID: 34619098; PMCID: PMC8489881.
41. Pilishvili T, Fleming-Dutra KE, Farrar JL, Gierke R, Mohr NM, Talan DA, Krishnadasan A, Harland KK, Smithline HA, Hou PC, Lee LC, Lim SC, Moran GJ, Krebs E, Steele M, Beiser DG, Faine B, Haran JP, Nandi U, Schrading WA, Chinnock B, Henning DJ, LoVecchio F, Nadle J, Barter D, Brackney M, Britton A, Marceaux-Galli K, Lim S, Phipps EC, Dumyati G, Pierce R, Markus TM, Anderson DJ, Debes AK, Lin M, Mayer J, Babcock HM, Safdar N, Fischer M, Singleton R, Chea N, Magill SS, Verani J, Schrag S; Vaccine Effectiveness Among Healthcare Personnel Study Team. Interim Estimates of Vaccine Effectiveness of Pfizer-BioNTech and Moderna COVID-19 Vaccines Among Health Care Personnel - 33 U.S. Sites, January-March 2021. MMWR Morb Mortal Wkly Rep. 2021 May 21;70(20):753-758. doi: 10.15585/mmwr.mm7020e2. PMID: 34014909; PMCID: PMC8136422.
42. Tenforde MW, Olson SM, Self WH, Talbot HK, Lindsell CJ, Steingrub JS, Shapiro NI, Ginde AA, Douin DJ, Prekker ME, Brown SM, Peltan ID, Gong MN, Mohamed A, Khan A, Exline MC, Files DC, Gibbs KW, Stubblefield WB, Casey JD, Rice TW, Grijalva CG, Hager DN, Shehu A, Qadir N, Chang SY, Wilson JG, Gaglani M, Murthy K, Calhoun N, Monto AS, Martin ET, Malani A, Zimmerman RK, Silveira FP, Middleton DB, Zhu Y, Wyatt D, Stephenson M, Baughman A, Womack KN, Hart KW, Kobayashi M, Verani JR, Patel MM; IVY Network; HAIVEN Investigators. Effectiveness of Pfizer-BioNTech and Moderna Vaccines Against COVID-19 Among Hospitalized Adults Aged ≥65 Years -

United States, January-March 2021. MMWR Morb Mortal Wkly Rep. 2021 May 7;70(18):674-679. doi: 10.15585/mmwr.mm7018e1. PMID: 33956782.

43. Yun C, Lee HJ, Lee CJ. Small Molecule Drug Candidates for Managing the Clinical Symptoms of COVID-19: a Narrative Review. Biomol Ther (Seoul). 2021 Oct 7. doi: 10.4062/biomolther.2021.134. Epub ahead of print. PMID: 34615772.

Tables

Table 1. Prevalence of SARS-CoV-2 lineages from April 2021 to October 2022.

WHO label	Alpha	Beta	Gamma	Delta	Lambda	Eta	Theta	Omicron	None
Pango Lineage	B.1.1.7	B.1.351	P.1	B.1.617.2*	C.37	B.1.525	P.3	B.1.1.529°	A.27
April	88.8%	-	5.6%	-	-	5.6%	-	-	-
May	94.1%	-	-	-	-	4.4%	-	-	1.5%
June	96%	0,8%	1.6%	-	1.6%	-	-	-	-
July	12.2%	-	2%	85.5%	-	-	0.3%	-	-
August	1,20%	0.1%	0.3%	98%	0.4%	-	-	-	-
September	0.2%	-	-	99.8%	-	-	-	-	-
October	-	-	-	100%	-	-	-	-	-
November	-	-	-	100%	-	-	-	-	-
December	-	-	-	83%	-	-	-	17%	-
January/22	-	-	-	23.1%	-	-	-	76.9%	-
February	-	-	-	6.5%	-	-	-	93.5%	-
March	-	-	-	-	-	-	-	100%	-
April	-	-	-	-	-	-	-	100%	-
May	-	-	-	-	-	-	-	100%	-
June	-	-	-	-	-	-	-	100%	-
July	-	-	-	-	-	-	-	100%	-
August	-	-	-	-	-	-	-	100%	-
September	-	-	-	-	-	-	-	100%	-
October	-	-	-	-	-	-	-	100%	-

*****B.1.617.2 and parent lineages; ° B.1.1.529 and parent lineages

Table 2a. Mutations in nsp12 from April 2021 to December 2021.

Mutations (%) \ Months (n.)	April (n.18)	May (n.70)	June (n.127)	July (n.335)	August (n.698)	September (n.550)	October (n.358)	November (n.508)	December (n.560)
S6L*	-	-	-	-	2 (0.3%)	-	-	-	-
T26I*	-	-	-	-	-	-	-	-	2 (0,35%)
S27I	-	-	-	-	-	-	-	-	-
Y32N*	-	-	-	-	1 (0.1%)	-	-	-	-
G44S°	-	-	-	-	-	-	-	-	-
A46S *	-	-	-	5 (1.5%)	6 (0.9%)	1 (0.2%)	5 (1.4%)	-	-
K59N†	-	-	-	1 (0.3%)	-	-	-	-	-
K59R*	-	-	-	1 (0.3%)	-	-	-	-	-
E61D*	-	-	-	-	-	1 (0.2%)	-	-	-
E61Q	-	-	-	-	-	-	-	-	-
K91R°	-	-	-	-	-	-	-	-	-
P94L°	-	-	-	-	-	-	-	-	-
D107N*	-	-	-	-	-	-	-	2 (0.4%)	3 (0,53%)
D140Y*	-	-	-	-	-	-	-	1 (0,2%)	-
L146F*	-	-	-	-	-	-	-	1 (0,2%)	-
D153Y									
W162C*	-	-	-	-	-	-	-	-	2 (0,35%)
R197Q*	-	-	-	13 (3.9%)	20 (2.9%)	2 (0.4%)	1 (0.3%)	24 (4,7%)	39 (7.6%)
N215D°	-	-	-	-	-	-	-	-	2 (0,35%)
N215Y	-	-	-	1 (0.3%)	-	-	-	-	-
I223V°	-	-	-	-	-	-	-	-	-
T248I°	-	-	-	-	-	-	-	-	-
R249M*	-	-	-	-	2 (0.3%)	-	-	-	-
S255A*	-	-	-	-	-	-	-	1 (0,2%)	-
V257F*	-	-	-	-	-	-	-	2 (0.4%)	-
K263R*	-	-	-	-	-	-	2 (0.6%)	-	-
I266V	-	-	-	-	-	-	-	-	-
T293I*	-	-	-	-	-	-	-	1 (0,2%)	-
P323L #*‡§ϕ°	16 (88.9%)	63 (90%)	107 (84.2%)	317 (94.6%)	647 (92.6%)	458 (83.3%)	314 (87.7%)	442 (87%)	485 (86,4%)
S325I	-	-	-	-	-	-	-	-	-
V330A*	-	-	-	-	-	-		-	1 (0,2%)
Q357H*	-	-	-	-	-	-	1 (0.3%)	8 (1.6%)	4 (0.7%)
Y346D*	-	-	-	-	-	1 (0.2%)	-	-	-
M380I*	-	-	-	-	-	-		1 (0,2%)	8 (1,4%)
S384P*	-	-	-	7 (2.1%)	2 (0.3%)	-	-	-	-
A406V*	-	-	-	-	-	-	-	-	2 (0,4%)
P412S*	-	-	-	-	-	-	-	2 (0.4%)	3 (0,5%)
A423V*	-	-	-	-	-	-	-	-	15 (2,7%)
P461S*	-	-	-	-	-	-	-	3 (0.6%)	6 (1%)
M463I*	-	-	-	2 (0.6%)	1 (0.1%)	-	-	17 (3,3%)	3 (0,5%)
V472L*	-	-	-	-	-	7 (1.3%)	20 (5.6%)	7 (1,4%)	-
K478N*	-	-	-	-	-	1 (0.2%)	-	-	-
D481A*	-	-	-	-	-	-	-	1 (0,2%)	1
V587L†	-	-	-	1 (0.3%)	-	-	-	-	-
V605F*	-	-	-	-	-	-	1 (0.3%)	-	-
D608G*	-	-	-	-	-	-		-	6 (1%)
H613Y*	-	-	-	-	2 (0.3%)	1 (0.2%)	-	-	-
D615I*	-	-	-	-	-	-	-	-	-
V637I*	-	-	-	-	-	1 (0.2%)	-	-	-
T644M*	-	-	-	-	-	1 (0.2%)	-	-	-
R651C*	-	-	-	-	1 (0.1%)	-	-	-	-
A656V*	-	-	-	5 (1.5%)	9 (1.3%)	5 (0.9%)	1 (0.3%)	-	-
G671S*°	-	-	-	284 (84.8%)	666 (95.4%)	535 (97.3%)	352 (98.3%)	507 (99,8%)	462 (82,5%)
A685S*	-	-	-	-	2 (0.3%)	4 (0.7%)	-	-	-
C697F*	-	-	-	-	-	-	-	1 (0,2%)	-
L707V*	-	-	-	-	-	-	2 (0.6%)	-	-
A716V#	10 (55.6%)	4 (5.7%)	2 (1.6%)	-	-	-	-	-	-
H725Y*	-	-	-	-	-	-	-	1 (0,2%)	5 (0,9%)
D738Y°	-	-	-	-	-	-	-	-	-
E744D*	-	-	-	-	-	-	-	3 (0,6%)	-
H752D°	-	-	-	-	-	-	-		
M756I*	-	-	-	-	-	1 (0.2%)	-	1 (0,2%)	-
S772F*	-	-	-	-	-	6 (1.1%)	-	1 (0,2%)	-
S795F*	-	-	-	-	-	1 (0.2%)	-	-	-
T803I*	-	-	-	-	-	-	-	-	-
D804N*	-	-	-	-	-	-	-	16 (3,1%)	10 (1,8%)
T806A°	-	-	-	-	-	-	-	-	1 (0,2%)
H810R									
Q822H*	-	-	-	4 (1.2%)	28 (4%)	33 (6%)	24 (6.7%)	25 (4,9%)	26 (4,6%)
D824Y*	-	-	-	3 (0.9%)	13 (1.9%)	5 (0.9%)	-	-	-
P830S	-	-	-	-	-	-	-	-	-
Y831C	-	-	-	-	-	-	-	-	-
S835P°	-	-	-	-	-	-	-	-	-
T853P°	-	-	-	-	-	-	-	-	-
L838I*	-	-	-	51 (15.2%)	190 (27.2%)	66 (12%)	63 (17.6%)	26 (5,1%)	37 (6.6%)
Q875R°	-	-	-	-	-	-	-	-	1 (0,2%)
Y877C*	-	-	-	1 (0.3%)	1 (0.1%)	-	6 (1.7%)	-	-
A878V*	-	-	-	1 (0.3%)	-	3 (0.5%)	-	-	-
H892N*	-	-	-	-	-	-	-	-	6 (1%)
M899I*	-	-	-	-	-	-	-	-	1 (0,2%)
L900F*	-	-	-	-	-	-	1 (0.3%)	-	-
V905A*	-	-	-	-	2 (0.3%)	-	-	-	-
del T908*	-	-	-	-	-	-	-	20 (3,9%)	6 (1%)
E922R	-	-	-	-	-	-	-	-	-

#B.1.1.7; *B.1.617.2 and parent lineages; †P.3; §P.1; ϕB.1.525; ‡B.1.351; °B.1.1.529

Table 2b. Mutations in nsp12 from January 2022 to October 2022.

Mutations (%) \ Months (n.)	January (n.363)	February (n.292)	March (n.52)	April (n.34)	May (n.8)	June (n.24)	July (n.39)	August (n.96)	October (n.23)
S6L*	-	-	-	-	-	-	-	-	-
T26I*	-	-	-	-	-	-	-	-	-
S27I	1 (0.3%)	-	-	-	-	-	-	-	-
Y32N*	-	-	-	-	-	-	-	-	-
G44S°	8(2.2%)	1 (0.3%)	-	-	-	-	-	-	-
A46S *	-	-	-	-	-	-	-	-	-
K59N†	-	-	-	-	-	-	-	-	-
K59R*	-	-	-	-	-	-	-	-	-
E61D*	-	-	-	-	-	-	-	-	-
E61Q	-	-	-	1 (2.9%)	-	-	-	-	-
K91R°	-	-	1 (1.9%)	-	-	-	-	-	-
P94L°	-	-	-	-	-	-	-	-	-
D107N*	-	1 (0.3%)	-	-	-	-	-	-	-
D140Y*	-	-	-	-	-	-	-	-	-
L146F*	-	-	-	-	-	-	-	-	-
D153Y			-	-	-	-	-	-	3 (13%)
W162C*	-	-	-	-	-	-	-	-	-
R197Q*	4 (1.1%)	1 (0.3%)	-	-	-	-	-	-	-
N215D°	-	-	-	-	-	-	-	-	-
N215Y	-	-	-	-	-	-	-	-	-
I223V°	-	4 (1.4%)	-	-	-	-	-	-	-
T248I°	-	-	1 (1.9%)	-	-	-	-	-	-
R249M*	-	-	-	-	-	-	-	-	-
S255A*	-	-	-	-	-	-	-	-	-
V257F*	-	-	-	-	-	-	-	-	-
K263R*	-	-	-	-	-	-	-	-	-
I266V	1 (0.3%)	-	-	-	-	-	-	-	-
T293I*	-	-	-	-	-	-	-	-	-
P323L#,*,†,§,ǂ,°	363 (100%)	282 (96.6%)	52 (100%)	34 (100%)	8 (100%)	24(100%)	39(100%)	96 (100%)	23 (100%)
S325I	-	-	-	-	-	-	-	1 (1%)	-
V330A*	-	-	-	-	-	-	-	-	-
Q357H*	-	-	-	-	-	-	-	-	-
Y346D*	-	-	-	-	-	-	-	-	-
M380I*	3 (0.8%)	-	-	-	-	-	-	-	-
S384P*	-	-	-	-	-	-	-	-	-
A406V*	-	-	-	-	-	-	-	-	-
P412S*	-	-	-	-	-	-	-	-	-
A423V*	3 (0.8%)	-	-	-	-	-	-	-	-
P461S*	1 (0.3%)	-	-	-	-	-	-	-	-
M463I*	2 (0.6%)	-	-	-	-	-	-	-	-
V472L*	-	-	-	-	-	-	-	-	-
K478N*	-	-	-	-	-	-	-	-	-
D481A*	-	-	-	-	-	-	-	-	-
V587L†	-	-	-	-	-	-	-	-	-
V605F*	-	-	-	-	-	-	-	-	-
D608G*	1 (0.3%)	-	-	-	-	-	-	-	-
H613Y*	-	-	-	-	-	-	-	-	-
D615I*	1 (0.3%)	-	-	-	-	-	-	-	-
V637I*	-	-	-	-	-	-	-	-	-
T644M*	-	-	-	-	-	-	-	-	-
R651C*	-	-	-	-	-	-	-	-	-
A656V*	-	-	-	-	-	-	-	-	-
G671S*°	80 (22%)	17 (5.8%)	-	-	-	-	2 (3.2%)	1 (1%)	-
A685S*	-	-	-	-	-	-	-	-	-
C697F*	-	-	-	-	-	-	-	-	-
L707V*	-	-	-	-	-	-	-	-	-
A716V#	-	-	-	-	-	-	-	-	-
H725Y*	-	-	-	-	-	-	-	-	-
D738Y°	-	-	1 (1.9%)	-	-	-	-	-	-
E744D*	-	2 (0.7%)	-	-	-	-	-	-	-
H752D°		1 (0.3%)	-	-	-	-	-	-	-
M756I*	-	-	-	-	-	-	-	-	-
S772F*	-	-	-	-	-	-	-	-	-
S795F*	-	-	-	-	-	-	-	-	-
T803I*	-	-	-	-	-	-	-	-	-
D804N*	-	-	-	-	-	-	-	-	-
T806A°	-	-	-	-	-	-	-	-	-
H810R			-	-	-	-	1 (1.6%)	-	-
Q822H*	-	-	-	-	-	-	-	-	-
D824Y*	-	-	-	-	-	-	-	-	-
P830S	-	-	-	-	-	-	-	-	1 (4.3%)
Y831C	-	-	1 (1.9%)	-	-	-	-	-	-
S835P°	1 (0.3%)	-	-	-	-	-	-	-	-
T853P°	-	1 (0.3%)	-	-	-	-	-	-	-
L838I*	23 (6.3%)	1 (0.3%)	-	-	-	-	-	-	-
Q875R°	2 (0.6%)	9 (3.1%)	8 (15.4%)	1 (2.9%)	-	-	-	-	-
Y877C*	-	-	-	-	-	-	-	-	-
A878V*	-	-	-	-	-	-	-	-	-
H892N*	-	-	-	-	-	-	-	-	-
M899I*	-	-	-	-	-	-	-	-	-
L900F*	-	-	-	-	-	-	-	-	-
V905A*	-	-	-	-	-	-	-	-	-
del T908*	-	-	-	-	-	-	-	-	-
E922R	-	-	-	-	-	-	-	1 (1%)	-

#B.1.1.7; *B.1.617.2 and parent lineages; †P.3; §P.1; ǂB.1.525; ‡B.1.351; °B.1.1.529

Table 3a. Mutations in nsp7 from April 2021 to December 2021.

Mutations (%) \ Months (n.)	April (n.18)	May (n.70)	June (n.127)	July (n.335)	August (n.698)	September (n.550)	October (n.358)	November (n.508)	December (n.560)
S1F*	-	-	-	-	-	-	1 (0.3%)	-	-
S1Y*	-	-	-	-	-	-	1 (0.3%)	-	-
M3I*	-	-	-	-	1 (0.1%)	-	-	-	-
K7R°	-	-	-	-	-	-	-	-	-
A30V*	-	-	-	-	-	-	1 (0.3%)	-	-
V33G°	-	-	-	-	-	-	-	-	-
V33A°	-	-	-	-	-	-	-	-	-
E47D#	-	-	-	-	1 (0.1%)	-	-	-	-
L56F*	-	-	-	1 (0.3%)	-	-	-	11 (2.2%)	5 (0.9%)
L60F*	-	-	-	1 (0.3%)	-	-	-	-	-
M62I*	-	-	-	-	-	-	1 (0.3%)	-	-
Q63H*	-	-	-	-	-	2 (0.4%)	-	-	-
L71F*†	-	-	-	1 (0.3%)	-	1 (0.2%)	-	-	1 (0.2%)
C72S*	-	-	-	1 (0.3%)	-	-	-	-	-

#B.1.1.7; *B.1.617.2 and parent lineages; †P.3; §P.1; ♄B.1.525; ‡B.1.351; °B.1.1.529

Table 3b. Mutations in nsp7 from January 2022 to October 2022.

Mutations (%) \ Months (n.)	January (n.363)	February (n.292)	March (n.52)	April (n.34)	May (n.8)	June (n.24)	July (n.39)	August (n.96)	October (n.23)
S1F*	-	-	-	-	-	-	-	-	-
S1Y*	-	-	-	-	-	-	-	-	-
M3I*	-	-	-	-	-	-	-	-	-
K7R°	-	-	-	1 (2.9%)	-	-	1 (2.6%)	-	-
A30V*	-	-	-	-	-	-	-	-	-
V33G°	-	-	-	-	-	-	1 (2.6%)	-	-
V33A°	-	-	-	-	-	-	-	2 (2.1%)	-
E47D#	-	-	-	-	-	-	-	-	-
L56F*	-	-	-	-	-	-	-	-	-
L60F*	-	-	-	-	-	-	-	-	-
M62I*	-	-	-	-	-	-	-	-	-
Q63H*	-	-	-	-	-	-	-	-	-
L71F*†	-	-	-	-	-	-	-	-	-
C72S*	-	-	-	-	-	-	-	-	-

#B.1.1.7; *B.1.617.2 and parent lineages; †P.3; §P.1; ♄B.1.525; ‡B.1.351; °B.1.1.529

Table 4a. Mutations in nsp8 from April 2021 to December 2021.

Mutations (%) \ Months (n.)	April (n.18)	May (n.70)	June (n.127)	July (n.335)	August (n.698)	September (n.550)	October (n.358)	November (n.508)	December (n.560)
N28S*	-	-	-	-	-	-	-	#VALORE!	1 (0.2%)
D30G*	-	-	-	-	1 (0.1%)	-	-	-	-
E30D°	-	-	-	-	-	-	-	-	-
V34F#	-	-	2 (1.6%)	-	-	-	-	-	-
A45S*	-	-	-	-	1 (0.1%)	-	-	-	-
R51C*	-	-	-	-	-	-	-	-	1 (0.2%)
M55I*	-	-	-	-	-	-	-	26 (5.1%)	8 (1.4%)
Q73R*	-	-	-	-	2 (0.3%)	-	-	-	-
A74V§	1 (5.6%)	-	-	-	-	-	-	-	-
T84I°	-	-	-	-	-	-	-	-	-
T93I*	-	-	-	1 (0.3%)	-	-	-	-	-
N105S#	-	-	1 (0.8%)	-	-	-	-	-	-
T123I*	-	-	-	-	1 (0.1%)	6 (1.1%)	-	-	1 (0.2%)
T123A*	-	-	-	-	-	-	1 (0.3%)	-	-
N140D*	-	-	-	-	-	-	1 (0.3%)	-	-
T145I°	-	-	-	-	-	-	-	-	1 (0.2%)
T148I*+	-	-	2 (1.6%)	4 (1.2%)	8 (1.1%)	1 (0.2%)	-	2 (0.4%)	14 (2.5%)
E155A#	-	-	-	-	1 (0.1%)	-	-	-	-
Q158H*	-	-	-	-	-	-	2 (0.6%)	-	-
V159F*	-	-	-	1 (0.3%)	-	-	-	-	-
V167A°	-	-	-	-	-	-	-	-	-
L169F*	-	-	-	-	3 (0.4%)	-	-	-	-
S170I#	-	-	-	-	1 (0.1%)	-	-	-	-
I185V*	-	-	-	-	-	1 (0.2%)	-	-	-

#B.1.1.7; *B.1.617.2 and parent lineages; †P.3; §P.1; ɸB.1.525; ‡B.1.351; °B.1.1.529

Table 4b. Mutations in nsp8 from January 2022 to October 2022.

Mutations (%) \ Months (n.)	January (n.363)	February (n.292)	March (n.52)	April (n.34)	May (n.8)	June (n.24)	July (n.39)	August (n.96)	October (n.23)
N28S*	1 (0.3%)	-	-	-	-	-	-	-	-
D30G*	-	-	-	-	-	-	-	-	-
E30D°	-	-	-	-	-	1 (4.2%)	-	-	-
V34F#	-	-	-	-	-	-	-	-	-
A45S*	-	-	-	-	-	-	-	-	-
R51C*	-	-	-	-	-	-	-	-	-
M55I*	-	-	-	-	-	-	-	-	-
Q73R*	-	-	-	-	-	-	-	-	-
A74V§	-	-	-	-	-	-	-	-	-
T84I°	-	1 (0.3%)	-	-	-	-	-	-	-
T93I*	-	-	-	-	-	-	-	-	-
N105S#	-	-	-	-	-	-	-	-	-
T123I*	-	-	-	-	-	-	-	-	-
T123A*	-	-	-	-	-	-	-	-	-
N140D*	-	-	-	-	-	-	-	-	-
T145I°	-	-	-	-	-	-	-	-	-
T148I*+	2 (0.6%)	-	-	-	-	-	-	-	-
E155A#	-	-	-	-	-	-	-	-	-
Q158H*	-	-	-	-	-	-	-	-	-
V159F*	-	-	-	-	-	-	-	-	-
V167A°	1 (0.3%)	-	-	-	-	-	-	-	-
L169F*	-	-	-	-	-	-	-	-	-
S170I#	-	-	-	-	-	-	-	-	-
I185V*	-	-	-	-	-	-	-	-	-

#B.1.1.7; *B.1.617.2 and parent lineages; †P.3; §P.1; ɸB.1.525; ‡B.1.351; °B.1.1.529

Table 5a. Mutations in nsp5 from April 2021 to December 2021.

Mutations (%) \ Months (n.)	April (n.18)	May (n.70)	June (n.127)	July (n.335)	August (n.698)	September (n.550)	October (n.358)	November (n.508)	December (n.560)
G15S[+]	-	-	2 (1.6%)	-	3 (0.4%)	-	-	-	-
M17I*#	-	-	1 (0.8%)	-	3 (0.4%)	-	-	-	-
M17V#	-	1 (1.4%)	-	-	-	-	-	-	-
N65S*	-	-	-	-	-	-	-	1 (0,2%)	-
K90R*#°	-	-	1 (0.8%)	8 (3.4%)	11 (1.6%)	10 (1.8%)	28 (7.8%)	46 (9.1%)	10 (1,8%)
T93I*	-	-	-	-	-	-	1 (0.3%)	-	-
A94T*	-	-	-	-	-	6 (1.1%)	-	-	-
A94V#	-	1 (1.4%)	-	-	-	-	-	-	-
P96S*	-	-	-	-	-	8	-	-	-
P96T*	-	-	-	-	-	4 (0.7%)	-	-	-
P108S°	-	-	-	-	-	-	-	-	-
V114L*	-	-	-	-	-	3 (0.5%)	-	-	-
P132H°	-	-	-	-	-	-	-	-	64 (11.4%)
V186F*	-	-	-	-	6 (0.9%)	122 (22.2%)	21 (5.9%)	8 (1.4%)	-
A191V*	-	-	-	-	-	-	-	-	-
T196M°	-	-	-	-	-	-	-	-	-
I213M*	-	-	5 (3.9%)	-	1 (0.1%)	-	-	-	-
L232I*	-	-	-	-	-	-	-	-	4 (0.7%)
L232F*	-	-	-	-	-	-	-	-	1 (0,2%)
A234V*	-	-	-	-	2 (0.3%)	-	-	-	-
Y239C*	-	-	-	-	-	-	-	-	1 (0,2%)
A260V*#	-	-	-	2 (0.6%)	-	-	-	6 (1.1%)	3 (0,5%)
M264I*	-	-	-	6 (1.8%)	-	-	-	-	-
M264V*	-	-	-	-	-	-	-	-	8 (1.4%)
N274H*	-	-	-	-	-	-	-	-	1 (0,2%)
T280N*	-	-	-	-	-	-	4 (1.1%)	-	-
T280I*	-	-	-	-	1 (0.1%)	-	-	-	-
E288D*	-	-	-	-	-	-	-	-	14 (2.5%)

#B.1.1.7; *B.1.617.2 and parent lineages; †P.3; §P.1; ᵠB.1.525; ‡B.1.351; °B.1.1.529

Table 5b. Mutations in nsp5 from January 2022 to October 2022.

Mutations (%) \ Months (n.)	January/22 (n.363)	February/22 (n.292	March/22 (n.52)	April/22 (n.34)	May/22 (n.8)	June/22 (n.24)	July/22 (n.39)	August/22 (n.96)	October/22 (n.23)
G15S[+]	-	-	-	-	-	-	-	-	-
M17I*#	-	-	-	-	-	-	-	-	-
M17V#	-	-	-	-	-	-	-	-	-
N65S*	-	-	-	-	-	-	-	-	-
K90R*#°	4 (1.1%)	-	-	-	-	-	-	-	-
T93I*	-	-	-	-	-	-	-	-	-
A94T*	-	-	-	-	-	-	-	-	-
A94V#	-	-	-	-	-	-	-	-	-
P96S*	-	-	-	-	-	-	-	-	-
P96T*	-	-	-	-	-	-	-	-	-
P108S°	-	1 (0.3%)	-	-	-	-	-	-	-
V114L*	-	-	-	-	-	-	-	-	-
P132H°	142 (39.1%)	224 (76.7%)	42 (80.8%)	22 (64.7%)	2 (25%)	19 (79.2%)	26 (66.7%)	63 (65.6%)	22 (95.7%)
V186F*	-	-	-	-	-	-	-	-	-
A191V*	1 (0.3%)	2 (0.7%)	-	-	-	-	-	-	-
T196M°	-	-	-	-	-	-	-	1 (1%)	-
I213M*	-	-	-	-	-	-	-	-	-
L232I*	-	-	-	-	-	-	-	-	-
L232F*	-	-	-	-	-	-	-	-	-
A234V*	-	-	-	-	-	-	-	-	-
Y239C*	-	-	-	-	-	-	-	-	-
A260V*#	-	-	-	-	-	-	-	-	-
M264I*	-	-	-	-	-	-	-	-	-
M264V*	-	-	-	-	-	-	-	-	-
N274H*	-	-	-	-	-	-	-	-	-
T280N*	-	-	-	-	-	-	-	-	-
T280I*	-	-	-	-	-	-	-	-	-
E288D*	4 (1.1%)	-	-	-	-	-	-	-	-

#B.1.1.7; *B.1.617.2 and parent lineages; †P.3; §P.1; ᵠB.1.525; ‡B.1.351; °B.1.1.529

Figures

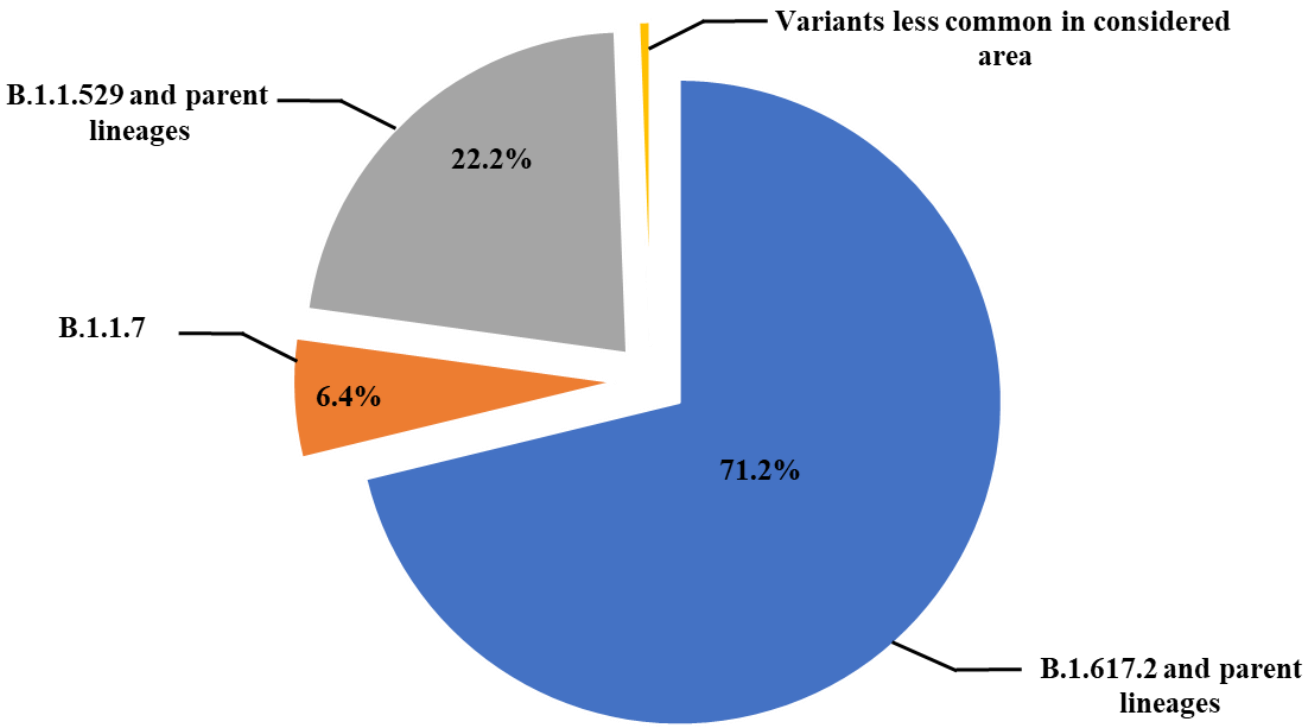

Figure 1. Schematic representation of SARS-CoV-2 lineages prevalence in 4,155 nasopharyngeal swabs from subjects with a first-time positive SARS-CoV-2 PCR test analyzed from April 2021 to October 2022.

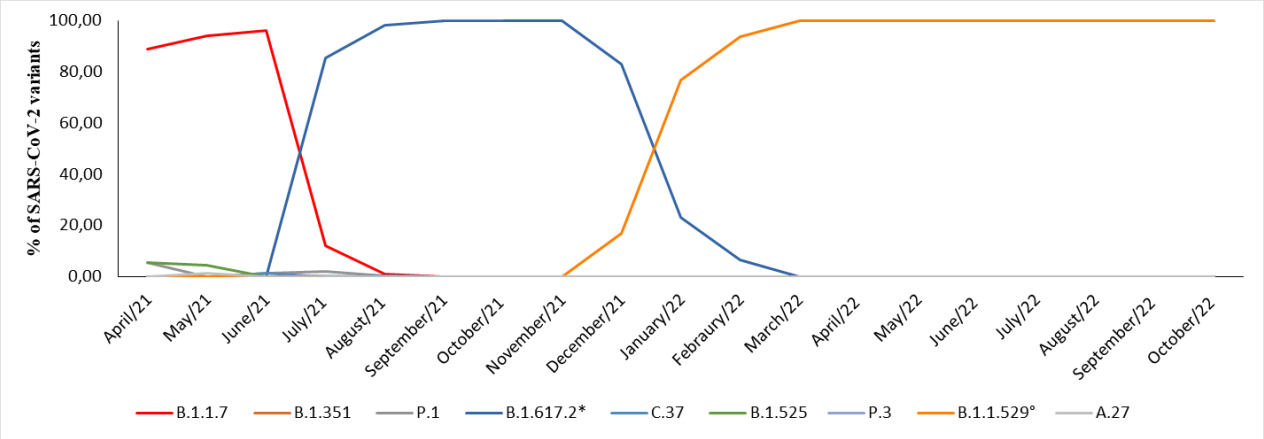

***B.1.617.2 and parent lineages; °B.1.1.529 and parent lineages**

Figure 2. Representation of prevalence of SARS-CoV-2 variants detected between April 2021 and October 2022. This image shows the rapid evolution of SARS-CoV-2 during the year and the emergence of new variants.

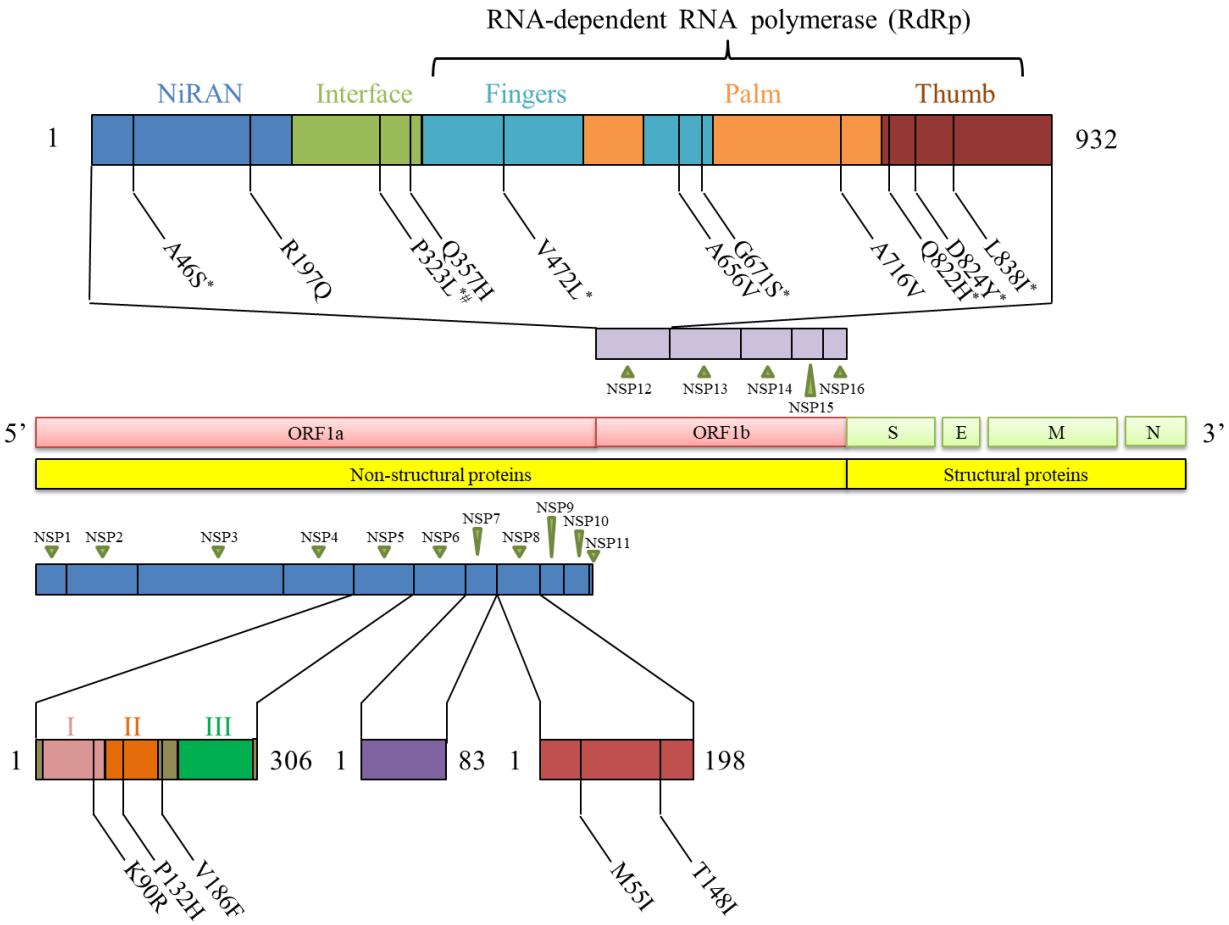

#B.1.1.7; *B.1.617.2 and parent lineages; †P.3; §P.1; ΦB.1.525; ‡B.1.351; °B.1.1.529

Figure 3. Schematic representation of the most frequent amino acid substitutions identified in nsp5, nsp7, nsp8, and nsp12.

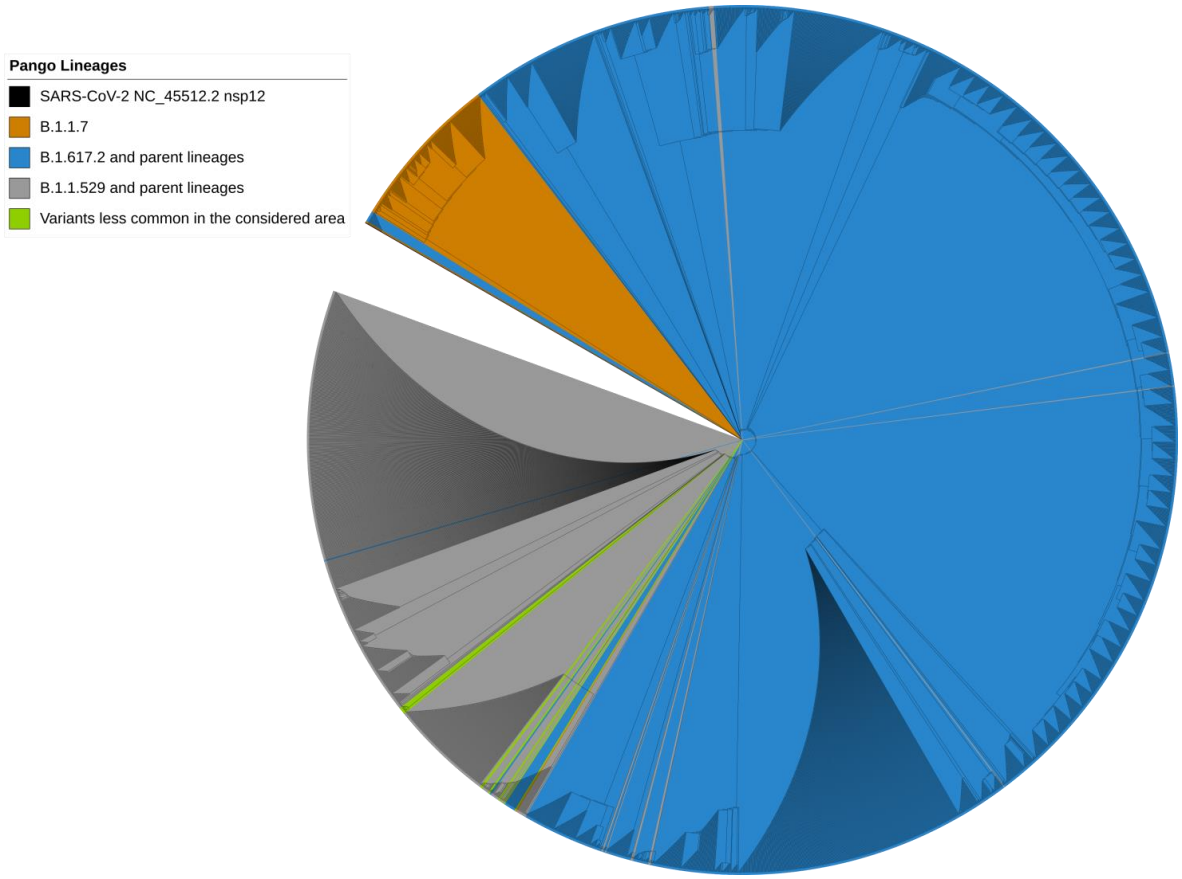

Figure 4. Phylogenetic tree of nsp12 showing evolutionary relationship between the samples analyzed and the reference sequence. The evolutionary history was inferred by using the Maximum Likelihood method and Tamura-Nei model.

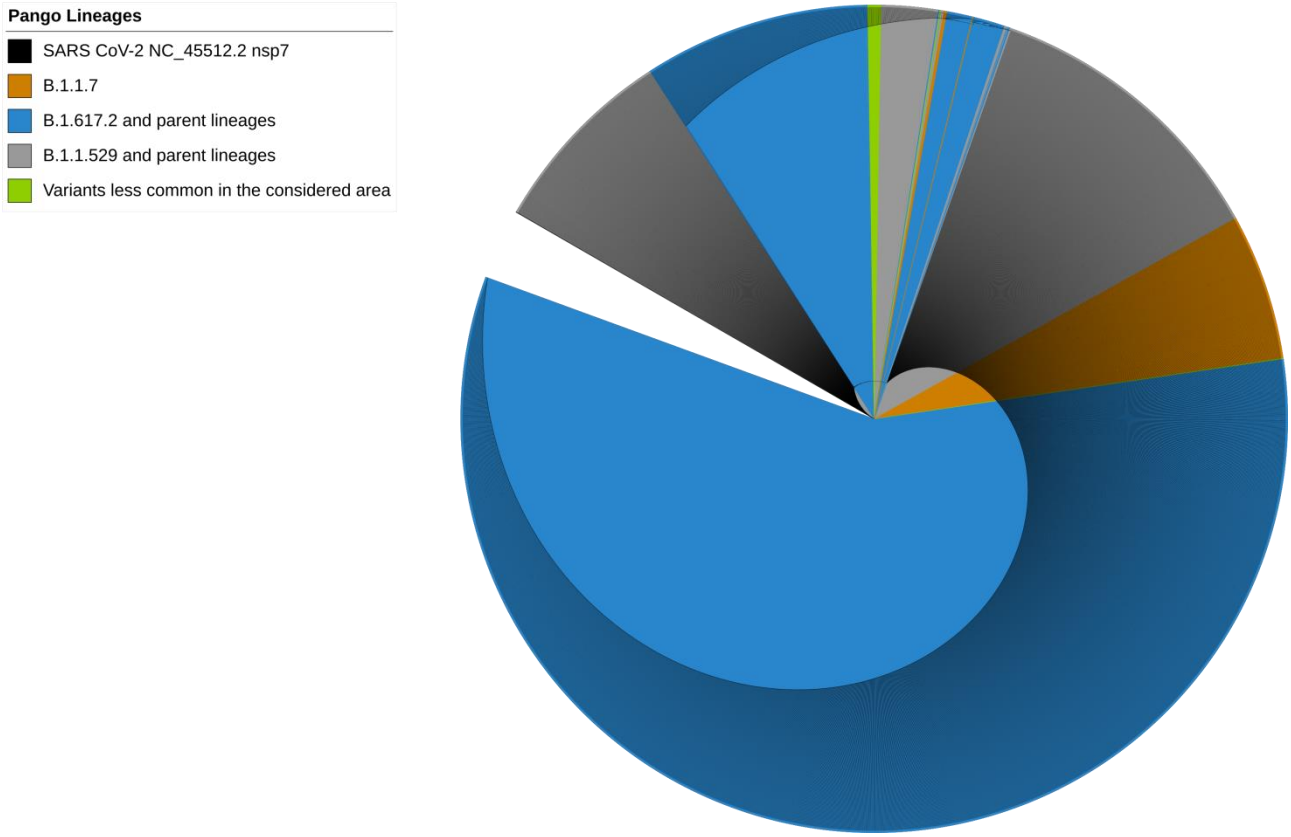

Figure 5. Phylogenetic tree of nsp7 showing evolutionary relationship between the samples analyzed and the reference sequence. The evolutionary history was inferred by using the Maximum Likelihood method and Tamura-Nei model.

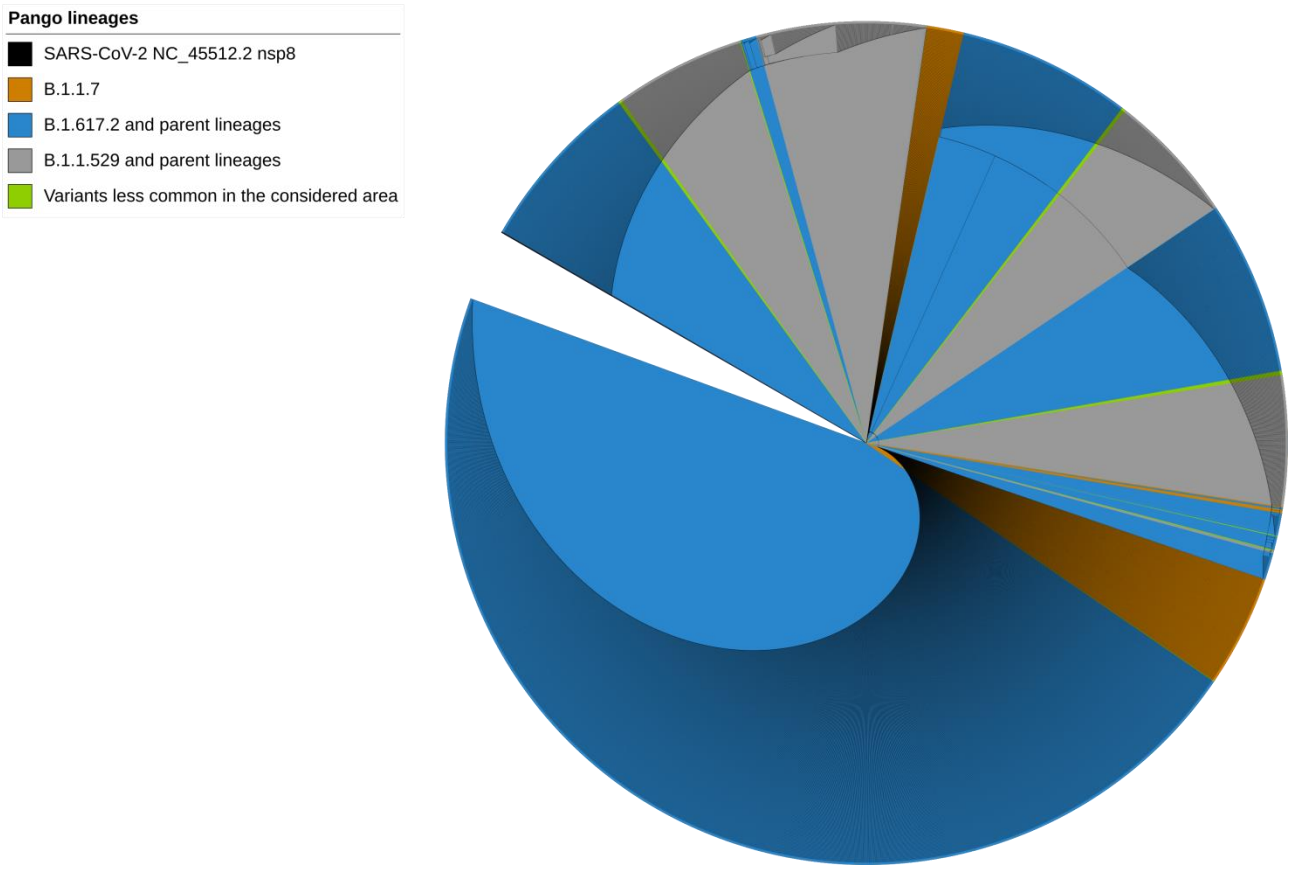

Figure 6. Phylogenetic tree of nsp8 showing evolutionary relationship between the samples analyzed and the reference sequence. The evolutionary history was inferred by using the Maximum Likelihood method and Tamura-Nei model.

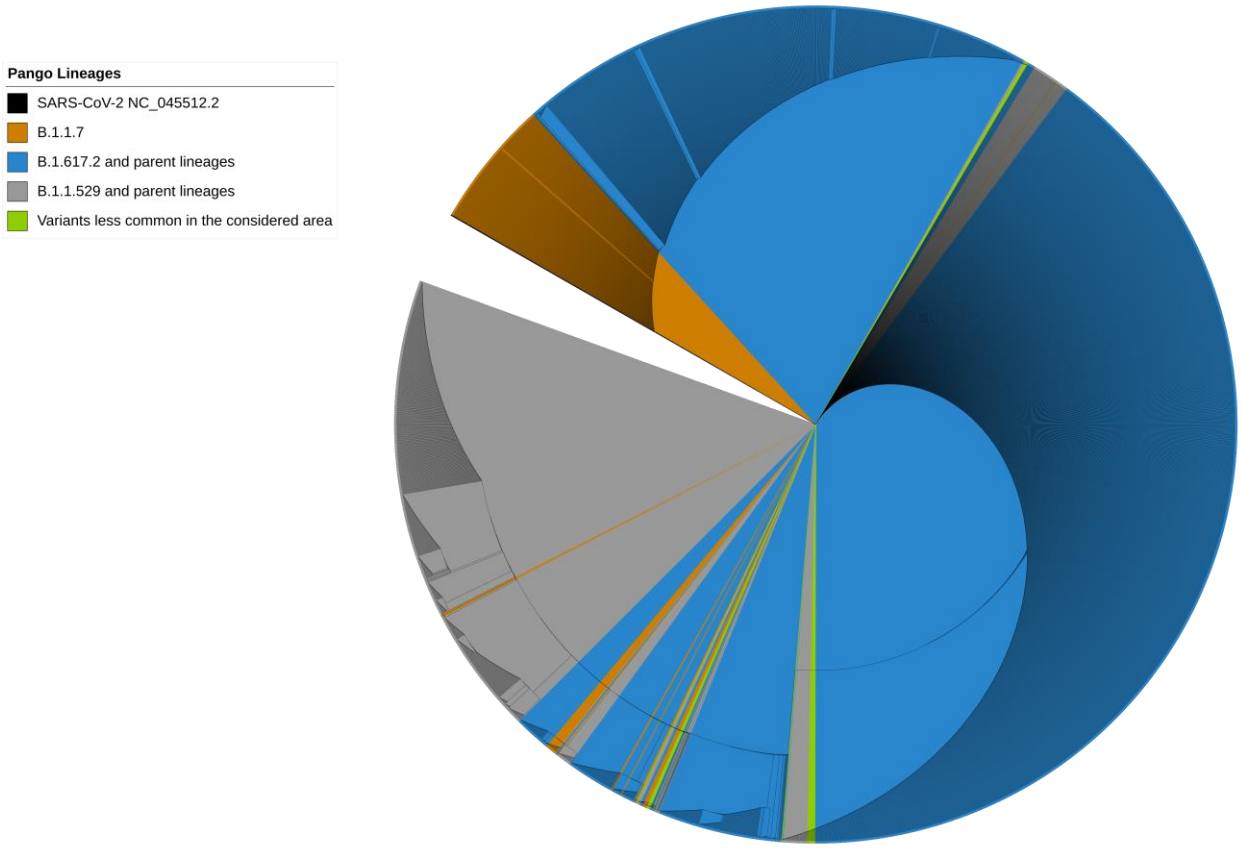

Figure 7. Phylogenetic tree of nsp5 showing evolutionary relationship between the samples analyzed and the reference sequence. The evolutionary history was inferred by using the Maximum Likelihood method and Tamura-Nei model.